

Partial Deoxygenative CO Homocoupling by a Diiron Complex

Devender Singh, Brian J. Knight, Vincent J. Catalano, Ricardo García-Serres,*
Vincent Maurel,* Jean-Marie Mouesca,* and Leslie J. Murray*

Abstract: One route to address climate change is converting carbon dioxide to synthetic carbon-neutral fuels. Whereas carbon dioxide to CO conversion has precedent in homo- and heterogeneous catalysis, deoxygenative coupling of CO to products with C–C bonds—as in liquid fuels—remains challenging. Here, we report coupling of two CO molecules by a diiron complex. Reduction of $\text{Fe}_2(\text{CO})_2\text{L}$ (**2**), where L^{2-} is a bis(β -diketiminato) cyclophane, gives $[\text{K}(\text{THF})_5][\text{Fe}_2(\text{CO})_2\text{L}]$ (**3**), which undergoes silylation to $\text{Fe}_2(\text{CO})(\text{COSiMe}_3)\text{L}$ (**4**). Subsequent C–OSiMe₃ bond cleavage and C=C bond formation occurs upon reduction of **4**, yielding $\text{Fe}_2(\mu\text{-CCO})\text{L}$. CO derived ligands in this series mediate weak exchange interactions with the ketenylidene affording the smallest *J* value, with changes to local metal ion spin states and coupling schemes (ferro- vs. antiferromagnetism) based on DFT calculations, Mössbauer and EPR spectroscopy. Finally, reaction of **5** with KEt_3BH or methanol releases the C_2O^{2-} ligand with retention of the diiron core

ing that, in concept, technologies that mediate deoxygenative CO homocoupling can open access to carbon-neutral liquid fuels. At present, the Fischer–Tropsch Process (FTP) facilitates this transformation, catalyzing the reaction of H₂ and CO to hydrocarbons using Fe, Co, or Ru catalysts.^[3–7] Various intermediates are proposed for FTP (e.g., hydroxycarbene), but mechanistic details remain unclear.^[5,8–11] For example, C–C bond formation is proposed to occur either between carbide-derived ligands (e.g., surface bound carbene) or hydroxycarbene, implying that even the order of CO deoxygenation, and C–C and C–H bond formation remain uncertain. Homogeneous systems competent for FTP-like reactions provide an alternate approach to studying reductive CO homocoupling and leverage solution-based spectroscopic methods. In addition, molecular systems have a potential advantage over the heterogeneous process: CO derived transients from an FTP-like reaction can serve as reactive species for novel chemical transformations or can be interfaced with other green technologies (i.e., renewable electricity) to minimize the environmental footprint. In this regard, Fe-based molecular systems are particularly attractive given the unique selectivity for olefins vs. alkanes as compared to other active metals.

Notably, CO homocoupling with deoxygenation and product release from iron centers without complex dissolution lacks precedent. Shriver and co-workers reported μ_3 -ketenylidene trinuclear metal carbonyl clusters $[\text{M}_3(\text{CO})_9(\mu_3\text{-CCO})]^{2-}$ ($\text{M}=\text{Fe}, \text{Ru}, \text{Os}$) with the CCO fragment derived from CO; functionalization and dissociation of the ketenylidene, however, has not been demonstrated (Figure 1).^[12,13] Kays' bis(aryl)iron(II) systems couple CO,^[14–16] but the CO coupling partners are limited to the aryl ligands, and Okazaki, et al. reported deoxygenative coupling of two μ_3 -CO ligands in $\text{Fe}_4(\mu_3\text{-CO})_4(\eta^5\text{-Cp}^1)$ clusters ($\text{Cp}^1=[\text{C}_5\text{H}_5]^-$ or $[\text{C}_5\text{H}_4\text{Me}]^-$) to a $\mu_4\text{-}(\eta^1\text{:}\eta^2\text{:}\eta^2\text{:}\eta^1)$ acetylene.^[17] Lastly, Atwood and co-workers generated low molecular weight hydrocarbons by reacting Cp-supported di- μ -CO diiron clusters with LiAlH₄,^[18] although the mechanism remains unclear. Extending to other metal complexes, Pampaloni's, Kawaguchi's, and Wolczanski's groups reported early *d*-block complexes for which CO deoxygenation affords ketenes, allenes, and μ -ethylidene and acetylene, respectively (Figure 1).^[13,19–22] Regenerating reactive complexes from the oxidometal products is a multistep process or is unreported. A similar outcome is reported for CO homologation by lanthanide metal-hydride clusters $\{\text{Cp}'\text{Ln}(\mu\text{-H})_2\}_4(\text{THF})$ ($\text{Cp}'=\text{C}_5\text{Me}_4\text{SiMe}_3$, and $\text{Ln}=\text{Y}, \text{Lu}$).^[23] Uniquely, reductive deoxygenative CO coupling by a terphenyl-diphosphine Mo complex from Agapie and co-workers,

Introduction

Carbon dioxide conversion to synthetic fuels can address climate change with minimal disruption to current transportation infrastructure. CO₂ conversion to CO has been reported for homo- and heterogeneous systems,^[1,2] suggest-

[*] D. Singh, B. J. Knight, L. J. Murray
Center for Catalysis and Florida Center for Heterocyclic Compounds

Department of Chemistry
University of Florida, Gainesville, FL (USA)
E-mail: murray@chem.ufl.edu

V. J. Catalano
Department of Chemistry
University of Nevada, Reno, NV (USA)

R. García-Serres
Université Grenoble Alpes, CNRS, CEA, IRIG, Laboratoire de Chimie et Biologie des Métaux
17 rue des Martyrs, 38000 Grenoble (France)
E-mail: ricardo.garcia@cea.fr

V. Maurel, J.-M. Mouesca
Université Grenoble Alpes, CEA, CNRS, IRIG, SyMMES, 38000 Grenoble (France)
E-mail: vincent.maurel@cea.fr
jean-marie.mouesca@cea.fr

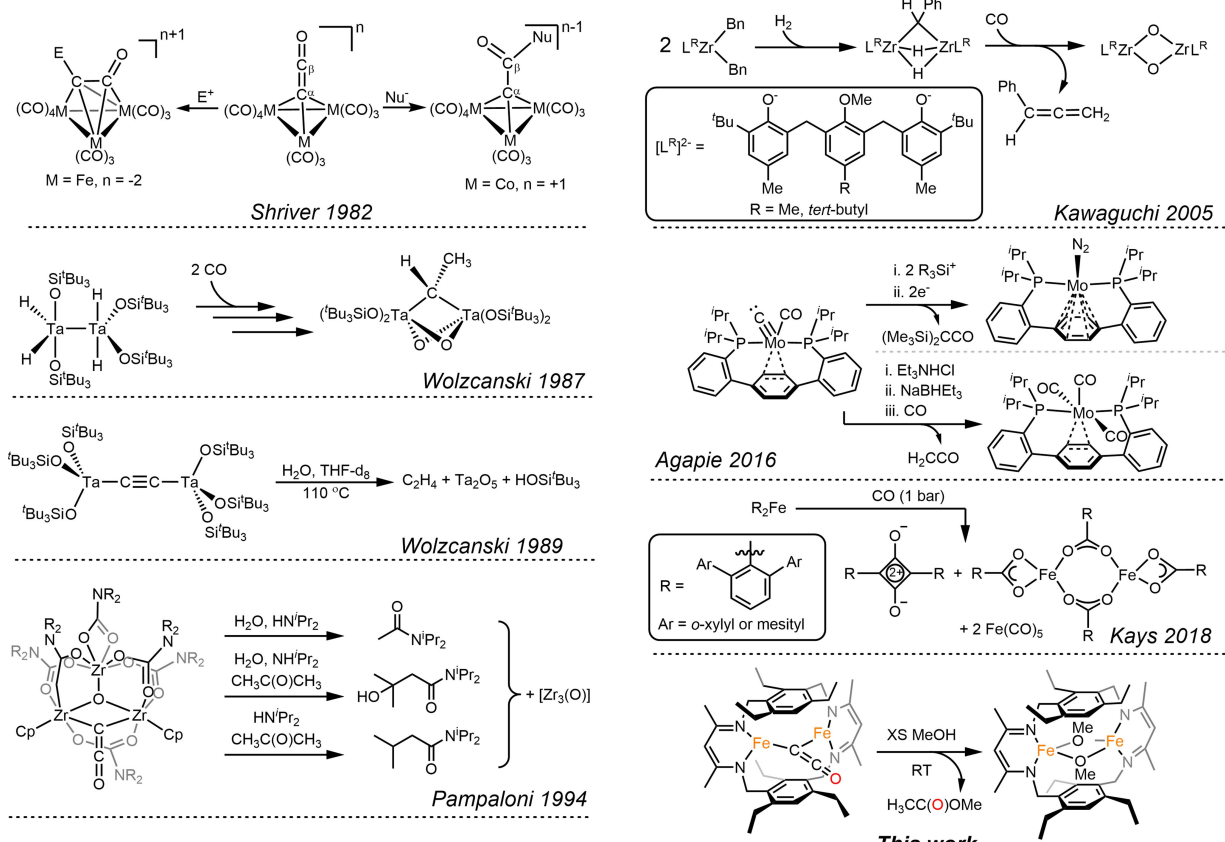


Figure 1. Prior reports of complexes competent for deoxygenative CO coupling.

liberates a reactive $\text{Mo}^0\text{-N}_2$ complex upon ketene release (Figure 1).^[24–26] Only H or trialkylsilyl-substituted ketenes are accessible, however, and reducing equivalents are required after the deoxygenation step to effect C–C bond formation and product release. Functionalization and dissociation of CO homologation products without complex degradation remain limited and rare, respectively.

We sought to effect FT-like transformations with CO coupling product release by mimicking the iron–iron cooperative effects in heterogeneous systems and those from the Shriver and Okazaki groups. Herein, we report that serial sequential reduction and silylation of a di(μ -carbonyl)diiron complex $\text{Fe}_2(\text{CO})_2\mathbf{L}$ (**2**) results in deoxygenative homologation of CO to yield a μ -ketenylidene diiron complex, $\text{Fe}_2(\mu\text{-CCO})\mathbf{L}$ (**5**). The sequence affords carbonyl, siloxycarbene, and ketenylidene complexes characterized by Mössbauer, EPR, and computational studies, which reveal weak metal–metal coupling mediated by unsaturated C donors and the sensitivity of local electronic configurations to reduction and bridging ligand identity. The μ -ketenylidene can be functionalized and released from **5** without decomposition of the diiron complex, which is a unique example of CO coupling and product release by a molecular iron system. As such, this system links the broad coupling chemistry of the polynuclear carbonyl clusters with the product release and complex recyclability of the early transition metal systems.

Results and Discussion

Treating the di(μ -hydrido)diiron(II) complex (**1-H**) with CO (1 atm) yields $\text{Fe}_2(\text{CO})_2\mathbf{L}$ (**2**) in good yield (82%, Scheme S1).^[27–29] IR absorptions for **2** at 1801, 1846, and 1856 cm^{-1} bathochromically shift for $\text{Fe}_2(^{13}\text{CO})_2\mathbf{L}$, suggesting related conformers in the solid state (Figure 2, S6–S7).^[28] Single-crystal X-ray diffraction (XRD) data reveal bridging and semi-bridging CO ligands and the pseudo- C_{2v} molecular symmetry from XRD agrees with ^1H NMR data.^[30] The formal diiron(I) core of **2** matches the smaller formal shortness ratio for the Fe–Fe distance,^[31] short Fe–C bonds (1.9056 Å), and the elongated C–O bonds in **2** (cf. free CO at 1.128 Å). The C–O bond lengths in **2** are comparable to precedent with phosphine or nitrosyl ligands.^[32–35] Mössbauer spectra of **1-H** and **2** recorded at 4.2 K or 5.8 K in applied magnetic fields indicate $S=0$ ground states resulting from antiferromagnetic coupling of paramagnetic centers. Determined isomer shift (δ) and quadrupole splitting (ΔE_Q) values suggest local high-spin (HS) iron(II) and iron(I) centers in **1-H** and **2**, respectively (Figure 3, S23);^[28,36–38] however, we have not considered effects such as rapid hydride motion.^[39] Using the Broken Symmetry (BS) methodology with the XRD structure of **2**, the coupling scheme is surprisingly sensitive to the method used (i.e. GGA, TPSSh or B3LYP) with computed ground states of either $S=4$ ($J_{\text{B3LYP}}=-38\text{ cm}^{-1}$) or $S=0$ ($J_{\text{TPSSh}}=+21\text{ cm}^{-1}$),

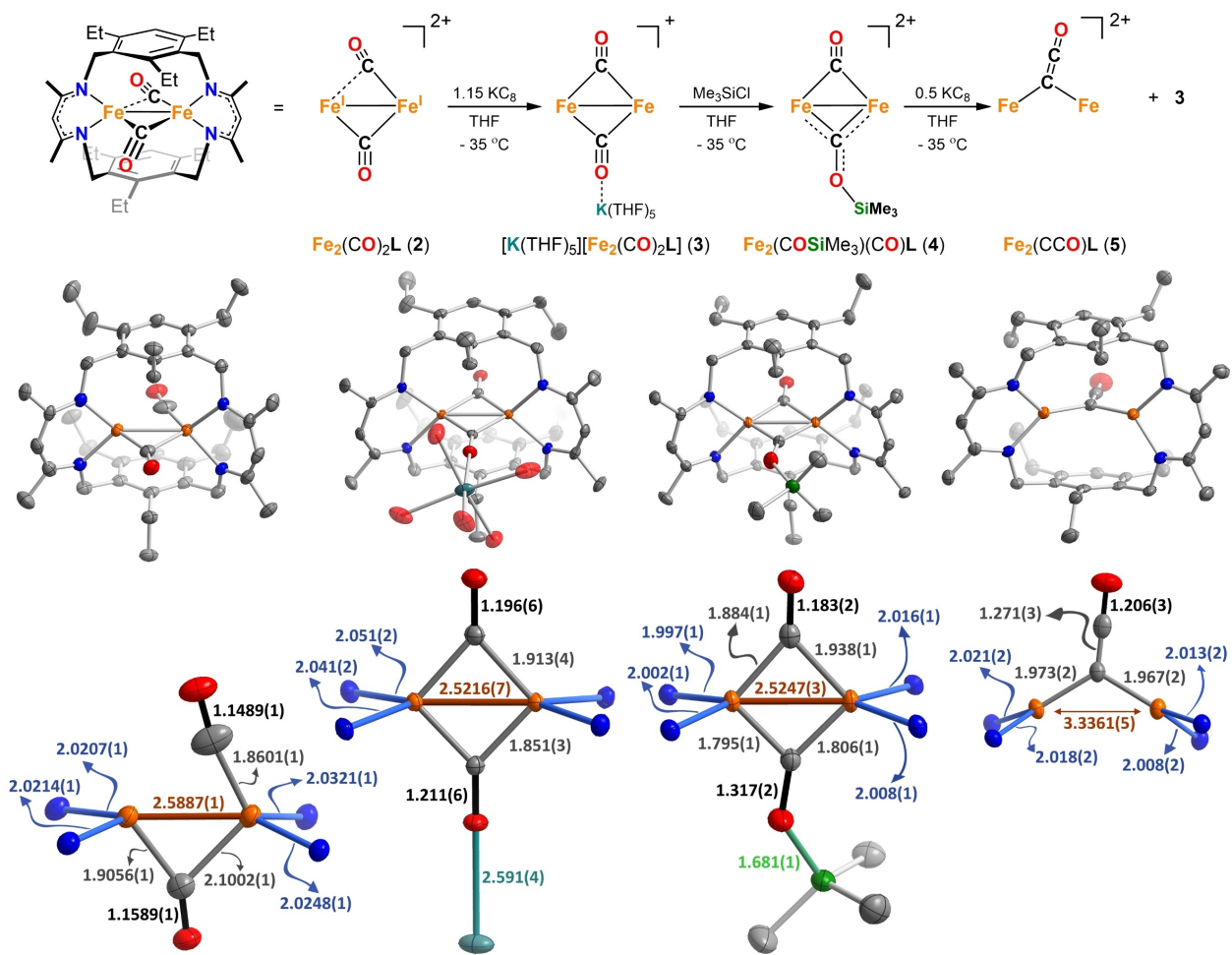


Figure 2. Top: Reaction scheme showing the synthesis of complexes **3–5**. Middle: XRD structures of **2–5** at 50% thermal ellipsoid from left to right, respectively. H atoms omitted for clarity and only O atoms for K⁺ bound THF molecules depicted. C, O, N, K, Si, and Fe atoms shown as gray, red, blue, teal, green, and orange ellipsoids, respectively. Bottom: Primary coordination spheres of Fe ions in **2–5** from left to right, with pertinent bond lengths in Å.

and $J_{\text{GGA-VBP}} = +269 \text{ cm}^{-1}$). CAS(16,12) calculations support AF-coupling in **2** with $J = +75.6 \text{ cm}^{-1}$, which is qualitatively consistent with the Mössbauer analysis above.^[40–42]

Treating **2** with KC₈ at -35°C yields **[K(THF)₅][Fe₂(CO)₂**L**] (**3**) with more activated CO ligands ($\nu_{\text{CO}} = 1700$ and 1809 cm^{-1}), which are of comparable energy to mononuclear anionic iron-carbonyl complexes with associated alkali cations (Figure 2, S9).^[33,43,44] XRD data on **3** confirm two μ -CO ligands and a **[K(THF)₅]⁺ cation bound to the more accessible or *exo* CO, which is more activated.^[33,45]****

We then sought to understand the electronic structure of **3**. Using the XRD coordinates, we computed energies for plausible spin states of **3**. The lowest energy state is the $M_s = 3/2$, implying an $S = 3/2$ ground state arising from the double exchange delocalizing mechanism between a HS $m_s = 1$ iron(0) and a low-spin $m_s = 1/2$ iron(I) (see SI). The local spin state change of the Fe^I from 3/2 to 1/2 upon reduction of the cluster evokes similar effects noted for larger clusters.^[46,47] Consistently, EPR spectra of **3** are axially anisotropic with $g_{\parallel} \approx 2$ and $g_{\perp} \approx 4$, supporting an $S = 3/2$ Kramer's doublet with a large zero-field splitting (ZFS) as

suggested by DFT computations ($D = 7.53 \text{ cm}^{-1}$). This spectrum was satisfactorily simulated with $E/D = 0.04$, which is quite close to the DFT computed E/D of 0.068 (Figure 4, Table S5). The 5.8 K Mössbauer spectrum of **3** displays a main doublet ($\approx 80\%$ total Fe) with a δ of 0.05 mm/s lower than that of **2** (Figure S23). Simulations of the applied-field spectra gave acceptable fits with an $S = 3/2$ spin Hamiltonian using ZFS parameters from EPR simulations and a hyperfine tensor comparable to other molecules in this series (Figure S25). The single observed quadrupole doublet in the low-field spectrum implies two equivalent Fe sites, as expected for valence delocalization by a double-exchange mechanism.

Reaction of **3** and Me₃SiCl affords **Fe**₂(CO)(COSiMe₃) (**4**) in excellent spectroscopic yield (Figure 2). The C–OSiMe₃ bond is intermediate between single and double bonds with a C–O–SiMe₃ bond angle of 138.7(2) $^\circ$. The Fe–CO bonds in **4** are comparable to those in **2** and short Fe–COSiMe₃ bonds indicate significant π -backdonation to both bridging ligands (Table S1).^[33,44,48–50] Indeed, the IR-active ν_{CO} in **4** observed at 1741 cm^{-1} is *more* activated than

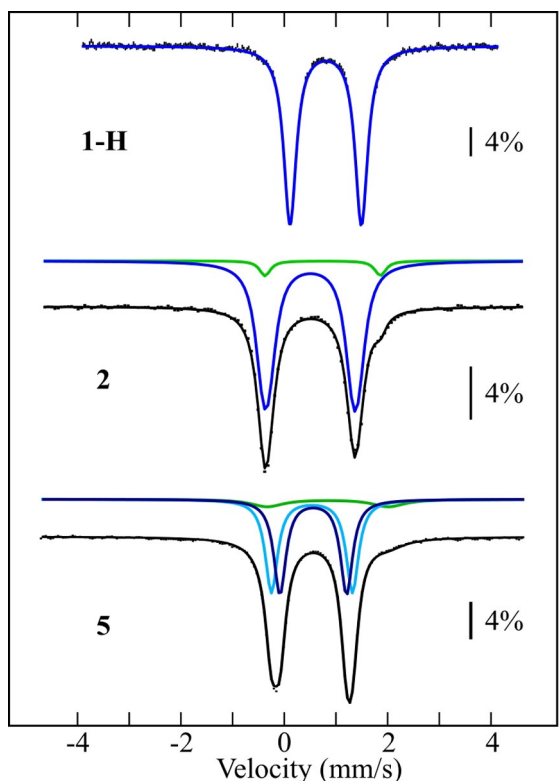


Figure 3. Mössbauer spectra of **1-H** at 4.2 K, and **2** and **5** at 5.8 K, in a 60 mT parallel applied magnetic field. Vertical error bars are experimental data points, coloured solid lines are individual quadrupole doublet simulations, and the black solid lines are the composite theoretical spectra. **1-H** contains only one doublet with parameters $\delta = 0.80 \text{ mm/s}$, $\Delta E_Q = 1.38 \text{ mm/s}$, and $\Gamma_{(\text{FWHM})} = 0.29 \text{ mm/s}$, characteristic of HS Fe^{II}.^[36–38] **2** contains a main doublet (blue line, 93 % total Fe) with $\delta = 0.51 \text{ mm/s}$, $\Delta E_Q = 1.73 \text{ mm/s}$ and $\Gamma = 0.34 \text{ mm/s}$, assigned to HS Fe^I,^[28] and a minor doublet (green line) assigned to a Fe^{II} impurity ($\delta/\Delta E_Q = 0.75/2.23 \text{ mm/s}$ and $\Gamma = 0.24 \text{ mm/s}$). **5** contains a symmetric main doublet with non-Lorentzian line profiles, which is well simulated with two equal-intensity quadrupole doublets of Lorentzian lines with (dark blue) $\delta = 0.56 \text{ mm/s}$, $\Delta E_Q = 1.29 \text{ mm/s}$, $\Gamma = 0.28 \text{ mm/s}$ and (light blue) $\delta = 0.53 \text{ mm/s}$, $\Delta E_Q = 1.57 \text{ mm/s}$, and $\Gamma = 0.29 \text{ mm/s}$, representing the two crystallographically inequivalent Fe^I sites. The green line is assigned to an Fe^{II} impurity ($\delta = 0.84 \text{ mm/s}$, $\Delta E_Q = 2.34 \text{ mm/s}$ and $\Gamma = 0.76 \text{ mm/s}$) for 10 % of total Fe.

in **2** (Figure S11). Finally, the short metal-metal separation (2.525(1) Å, FSR = 1.08) and contracted Fe–N_L distances imply minimal change to electron density at the metal centers upon silylation. Taken together, we infer a Fischer formalism for the [COSiMe₃] ligand with formally reduced metal centers in **4**.^[33,44,48,50] The first reductive redox process for **2** and **4** occur at a near coincident potential of –2.15 V vs. ferrocene/ferrocenium, hinting at redox leveling upon silylation (Figure S32).

As before, we surveyed the possible spin states of **4** computationally and determined the $M_s = 3/2$ state as the lowest in energy. Calculated Mulliken charge (–0.06) for the [COSiMe₃] fragment agrees with local $S=1$ Fe^{II} and $S=1/2$ Fe^I centers. Analogous to **3**, the EPR spectrum of **4** is axially anisotropic with $g_{\parallel} \approx 2$ and $g_{\perp} \approx 4$. This spectrum was satisfactorily simulated with $E/D = 0.03$, comparable to the

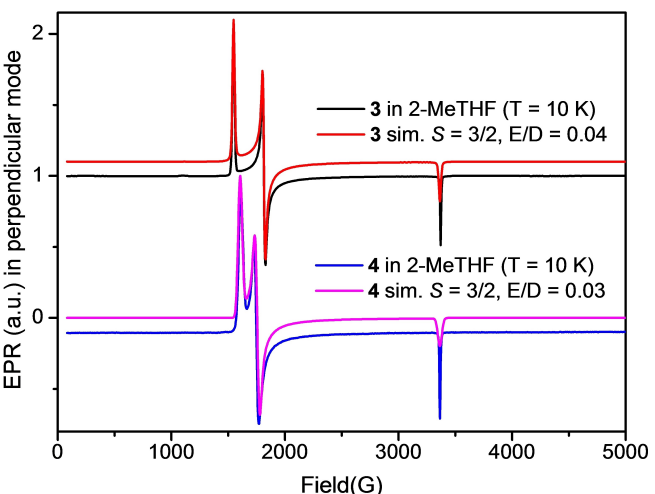


Figure 4. Perpendicular mode X-band EPR spectra of **3** and **4** at 10 K in 2-methyltetrahydrofuran. Simulations parameters for **3**: $S = 3/2$, $g = 2.067$, $D = 7.53 \text{ cm}^{-1}$, $E/D = 0.040$; and for **4**: $S = 3/2$, $g = 2.055$, $D = 8.20 \text{ cm}^{-1}$, $E/D = 0.030$.

$E/D = 0.057$ (with $D = 8.20 \text{ cm}^{-1}$) calculated by DFT methods (Figure 4).

The 82 K Mössbauer spectrum of **4** displays a single quadrupole doublet ($\delta/\Delta E_Q = 0.32/0.62 \text{ mm/s}$), indicating fully delocalized valences, *viz.* [Fe^{1.5+}]₂ (Figure S26). This isomer shift is in range of four-coordinate HS Fe^{III} centers in similar ligand environments,^[51–53] differing substantially from the value reported ($\delta = 0.81 \text{ mm/s}$) for $S = 3/2$ Fe centers in the [Fe^{1.5+}]₂ complex of this ligand, Fe₂Br₂(N₂)L.^[54] Given that δ varies not only with oxidation state (formally +1.5 for both complexes) but also with local spin ($s = 1/2$ vs. 3/2), we compared experimental δ values for **1-H** to **5** with calculated electron densities at the Fe nuclei. The good linear trend validates the computational results, supporting the local spin assignments in **4** (Figure S30). Simulating the applied field 2.3-K and 20-K Mössbauer spectra in the slow and fast relaxation limits, respectively, gave the best fit for an $S = 3/2$ spin Hamiltonian with the parameters noted in the figure caption (Figure 5, Table S5).

Reaction of **4** with 0.5 equiv. KC₈ gives a mixture of **3**, a C_{2v} symmetric species (**5**), and hexamethyldisiloxane (HMDSO) by ¹H NMR spectroscopy (Figure S12), the latter product implying C–OSiMe₃ bond scission. A 1991 cm^{–1} IR absorption in spectra of **5** is similar in energy to those for metal ketenylidenes, suggesting C–OSiMe₃ bond cleavage accompanied by C=C bond formation (Figure S13, S14).^[19,21,55] Consistently, XRD data confirm **5** as a (μ -ketenylidene)diiiron complex from C–OSiMe₃ bond cleavage and C=C bond formation (Figure 2). In the structure, each Fe is trigonal planar with Fe–CCO and Fe–N_L bond lengths comparable to those in **2**. We used the bond valence sum method to estimate iron oxidation states (~+1.3 for each Fe), hinting at carbene character for the CCO donor.^[56] Concomitant formation of **5** and **3** upon reduction of **4** could arise from competitive nucleophilic attack by the Me₃SiO[–] formed by reduction of **4** on the Si

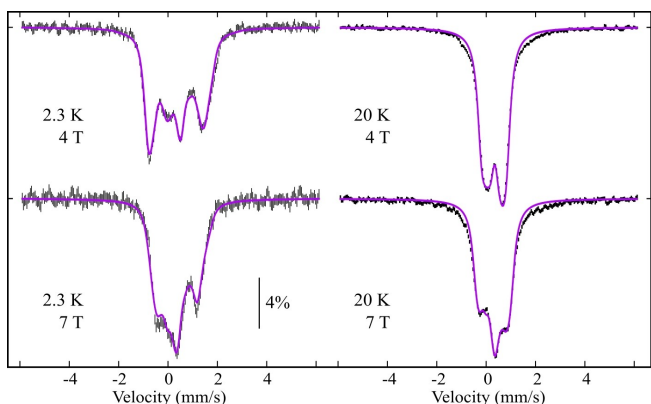


Figure 5. Mössbauer spectra of **4** under conditions noted with fields applied parallel to the gamma rays. Vertical bars are the experimental data points. The purple line is the $S=3/2$ spin Hamiltonian simulation with $\delta=0.33 \text{ mm/s}$, $D=6.13 \text{ cm}^{-1}$, $E/D=0.03$, $\Delta E_Q=0.65 \text{ mm/s}$, $\eta=0.50$ and $A/(g_n\beta_n)=(-22, -6, -8) \text{ T}$. The EFG tensor is rotated relative to the ZFS frame with Euler angles $\alpha=0$ and $\beta=58^\circ$, and the hyperfine coupling tensor is rotated relative to the ZFS frame with Euler angles $\alpha=30^\circ$ and $\beta=94^\circ$.

center in as-yet reduced siloxycarbene **4**, as proposed for a mononuclear Mo system.^[24] Thus, adding Me_3SiCl to this reduction reaction should, and does, improve the yield and purity of **5** as does reducing **6**, synthesized from **3** and bis(chlorodimethylsilyl)ethane.

We surveyed various plausible electronic structures for **5** by DFT methods using the XRD structures, and found the BS ($M_s=0$) state to be the lowest energy state (see Supporting Information). Spin population analysis of this state describes **5** as comprising two locally HS Fe^{II} centers. This result is not altered when the structure of **5** is geometry optimized (see Supporting Information). The Mössbauer spectrum of **5** displays a main doublet with $\delta=0.55 \text{ mm/s}$ and $\Delta E_Q=1.43 \text{ mm/s}$ (Figure 3), consistent with three-coordinate HS Fe^I centers. Surprisingly, applied-field Mössbauer spectra of **5** reveal a ~30% larger magnetic splitting than expected for a singlet spin state, suggesting that **5** cannot have a pure singlet ground state. The applied-field Mössbauer spectra can be fitted assuming an integer-spin ground state (i.e., $S=1, 2, \dots$), which yields weak, positive, and anisotropic hyperfine coupling tensors (Figure S27), suggesting a dominant contribution of dipolar and spin-orbit coupling (SOC) terms to the hyperfine interaction.^[57] Alternatively, these spectra can be fitted assuming two weakly coupled $S=2$ Fe centers, resulting in an $S=0$ ground state and thermally accessible spin multiplets (Figure S27, Table S2). The fit obtained in this manner with hyperfine and ZFS parameters constrained to the computational results yields a plausible fit to the data with $J=+2.2 \text{ cm}^{-1}$. Consistent with an integer spin system, perpendicular mode EPR spectra recorded on **5** yield negligible signal, whereas an intense broad feature centered at $g\approx14.8$ is observed in parallel mode (Figure S29). This could arise from an $S=2, 3$ or 4 species.

DFT, Mössbauer, and EPR data point to weakly coupled iron(II) centers but disagree on the magnitude of that

interaction. Using CASSCF calculations on the geometry-optimized structure to better estimate J , we obtain $J<+10 \text{ cm}^{-1}$ (Tables S7–S10). The ground states in all CAS calculations are not dominated by a single configuration, consistent with the discrepancy between DFT and spectroscopic results. The electronic structure of **5** is complicated and, with data presented on **2–4**, point to the ligand field and exchange interactions mediated by bridging C-atom donors bound to weak-field ligated Fe centers as sensitive to coordination number and d electron count of the metal center. The simplest holistic interpretation of all data is that **5** comprises two $S=2$ ferrous ions that are uncoupled or weakly interacting, with J likely over-estimated by computational methods. Consistent with calculations on **5** being uniquely challenged in this series of complexes, electron density calculated at the iron nuclei in **5** is the most sensitive to the method used of all complexes reported here (Figure S30). We note that computed J values for **2–5** are sensitive to the method used and reflect unexpectedly weak exchange coupling mediated by the bridging ligands.

Finally, reacting **5** with MeOH yields $\text{Fe}_2(\text{OMe})_2\text{L}^{\text{bis}}$ and methyl acetate, the latter confirmed by using ^{13}C labeled **5** (Figure S17, S18). Also, **5** reacts with KHBEt_3 to afford **1-H** as the major product in ^1H NMR spectra, albeit as a mixture. This report is the first example of an iron system that couples CO and releases the organic product to give a recyclable complex, suggesting that catalytic FTP-like molecular systems as attainable.

Electrophilic reactivity of the carbide in iron carbonyl clusters correlates to the carbide coordination number. For example, $[\text{Fe}_4(\mu_4\text{-C})(\text{CO})_{12}]^{2-}$ reacts with H^+ and H_2 to form C–H and/or Fe–H bonds,^[58,59] but no such reactivity is observed in the hexa- and pentairon clusters.^[60–62] The triiron cluster is isolable only as the ketenylidene complex, which reacts as a masked carbide.^[12] Lack of reactivity of porphyrin and phthalocyanin-supported (μ -carbido)diiron complexes opposes this trend, but may arise from steric effects or greater metal–carbide π -overlap in these compounds versus the carbonyl clusters.^[63–68] C–O cleavage in **4** results in formation of a CCO donor, implying that if a transient carbide is formed, the reactivity parallels the observed and calculated electrophilicity of the carbide in carbonyl clusters.^[69] Thus, the higher coordinate carbides in the nitrogenase cofactors and FTP catalysts may mediate electronic coupling that can vary dramatically with local d -electron counts, although lower coordinate carbides at or near the surface of FTP catalysts may open pathways to ketenylidene formation.

Conclusion

Here, we report partial deoxygenative CO homologation by a diiron system, from which the coupled ketenylidene product can be readily released for the diiron core by reaction with MeOH or hydride sources. Aspects of the electronic structures of compounds **2–5** are unprecedented and unexpected, including the weak coupling mediated by CO, $[\text{COSiMe}_3]^-$, and $[\text{C}_2\text{O}]^{2-}$ bridging ligands, hinting at

more complicated electronic structures afforded by unsaturated C donors in the presence of weak-field supporting ligands.

Supporting Information

The authors have cited additional references within the Supporting Information.^[70–90] Crystallographic information can be found online.^[91]

Acknowledgements

Authors acknowledge the National Institutes of Health (R01-GM123241 to LJM and DS), computational resources supported by the National Science Foundation (CHE-2102098 to LJM), IR INFRANALYTICS FR2054 (to LJM), and French National Research Agency (Labex ARCANE, CBH-EUR-GS, ANR-17-EURE-0003 to RGS, JMM and VM). LJM and DS thank W. Buratto, J. Torres, and T. John for assistance. The content is solely the responsibility of the authors and does not necessarily represent the official views of the National Institutes of Health.

Conflict of Interest

The authors declare no conflict of interest.

Data Availability Statement

The data that support the findings of this study are available in the supplementary material of this article.

Keywords: CO Coupling · Carbonyl Ligands · Electronic Structure · Iron · Metal-Metal Interactions

- [1] K. A. Grice, *Coord. Chem. Rev.* **2017**, *336*, 78–95.
- [2] J. Qiao, Y. Liu, F. Hong, J. Zhang, *Chem. Soc. Rev.* **2014**, *43*, 631–675.
- [3] H. Fisher, F. Tropsch, *Brennst.-Chem.* **1923**, *4*, 276–285.
- [4] A. Y. Khodakov, W. Chu, P. Fongarland, *Chem. Rev.* **2007**, *107*, 1692–1744.
- [5] E. de Smit, B. M. Weckhuysen, *Chem. Soc. Rev.* **2008**, *37*, 2758–2781.
- [6] H. Jahangiri, J. Bennett, P. Mahjoubi, K. Wilson, S. Gu, *Catal. Sci. Technol.* **2014**, *4*, 2210–2229.
- [7] H. Mahmoudi, M. Mahmoudi, O. Doustdar, H. Jahangiri, A. Tsolakis, S. Gu, M. Lech Wyszynski, *Biofuels Eng.* **2017**, *2*, 11–31.
- [8] G. P. Van Der Laan, A. A. C. M. Beenackers, *Catal. Rev. Sci. Eng.* **1999**, *41*, 255–318.
- [9] R. A. van Santen, A. J. Markvoort, I. a. W. Filot, M. M. Ghouri, E. J. M. Hensen, *Phys. Chem. Chem. Phys.* **2013**, *15*, 17038–17063.
- [10] O. R. Inderwildi, S. J. Jenkins, D. A. King, *J. Phys. Chem. C* **2008**, *112*, 1305–1307.
- [11] F. Romero-Sarria, L. F. Bobadilla, E. M. Jiménez Barrera, J. A. Odriozola, *Appl. Catal. B* **2020**, *272*, 119032.
- [12] D. F. Shriver, M. J. Sailor, *Acc. Chem. Res.* **1988**, *21*, 374–379.
- [13] F. Calderazzo, U. Englert, A. Guarini, F. Marchetti, G. Pampaloni, A. Segre, G. Tripepi, *Chem. Eur. J.* **1996**, *2*, 412–419.
- [14] H. R. Sharpe, A. M. Geer, L. J. Taylor, B. M. Gridley, T. J. Blundell, A. J. Blake, E. S. Davies, W. Lewis, J. McMaster, D. Robinson, D. L. Kays, *Nat. Commun.* **2018**, *9*, 3757.
- [15] W. J. Evans, J. W. Grate, L. A. Hughes, H. Zhang, J. L. Atwood, *J. Am. Chem. Soc.* **1985**, *107*, 3728–3730.
- [16] W. J. Evans, D. S. Lee, J. W. Ziller, N. Kaltsoyannis, *J. Am. Chem. Soc.* **2006**, *128*, 14176–14184.
- [17] M. Okazaki, T. Ohtani, M. Takano, H. Ogino, *Organometallics* **2004**, *23*, 4055–4061.
- [18] M. M. Harris, J. D. Atwood, M. E. Wright, G. O. Nelson, *Inorg. Chem.* **1982**, *21*, 2117–2118.
- [19] F. Calderazzo, U. Englert, A. Guarini, F. Marchetti, G. Pampaloni, A. Segre, *Angew. Chem. Int. Ed.* **1994**, *33*, 1188–1189.
- [20] R. E. LaPointe, P. T. Wolczanski, J. F. Mitchell, *J. Am. Chem. Soc.* **1986**, *108*, 6382–6384.
- [21] D. R. Neithamer, R. E. LaPointe, R. A. Wheeler, D. S. Richardson, G. D. Van Duyne, P. T. Wolczanski, *J. Am. Chem. Soc.* **1989**, *111*, 9056–9072.
- [22] T. Matsuo, H. Kawaguchi, *J. Am. Chem. Soc.* **2005**, *127*, 17198–17199.
- [23] T. Shima, Z. Hou, *J. Am. Chem. Soc.* **2006**, *128*, 8124–8125.
- [24] J. A. Buss, T. Agapie, *Nature* **2016**, *529*, 72–75.
- [25] J. A. Buss, T. Agapie, *J. Am. Chem. Soc.* **2016**, *138*, 16466–16477.
- [26] J. A. Buss, G. A. Bailey, J. Oppenheim, D. G. Vander Velde, W. A. I. Goddard, T. Agapie, *J. Am. Chem. Soc.* **2019**, *141*, 15664–15674.
- [27] Y. Yu, A. R. Sadique, J. M. Smith, T. R. Dugan, R. E. Cowley, W. W. Brennessel, C. J. Flaschenriem, E. Bill, T. R. Cundari, P. L. Holland, *J. Am. Chem. Soc.* **2008**, *130*, 6624–6638.
- [28] K. J. Anderton, B. J. Knight, A. L. Rheingold, K. A. Abboud, R. García-Serres, L. J. Murray, *Chem. Sci.* **2017**, *8*, 4123–4129.
- [29] J. C. Ott, C. K. Blasius, H. Wadeohl, Lutz. H. Gade, *Inorg. Chem.* **2018**, *57*, 3183–3191.
- [30] R. J. Klingler, W. M. Butler, M. D. Curtis, *J. Am. Chem. Soc.* **1978**, *100*, 5034–5039.
- [31] F. A. Cotton, S. Koch, M. Millar, *J. Am. Chem. Soc.* **1977**, *99*, 7372–7374.
- [32] J. L. Kisko, T. Hascall, G. Parkin, *J. Am. Chem. Soc.* **1998**, *120*, 10561–10562.
- [33] Y. Lee, J. C. Peters, *J. Am. Chem. Soc.* **2011**, *133*, 4438–4446.
- [34] J. Rittle, J. C. Peters, *Proc. Natl. Acad. Sci. USA* **2013**, *110*, 15898–15903.
- [35] C.-Y. Lu, W.-F. Liaw, *Inorg. Chem.* **2013**, *52*, 13918–13926.
- [36] Y. Lee, K. J. Anderton, F. T. Sloane, D. M. Ermert, K. A. Abboud, R. García-Serres, L. J. Murray, *J. Am. Chem. Soc.* **2015**, *137*, 10610–10617.
- [37] A. Albers, S. Demeshko, K. Pröpper, S. Dechert, E. Bill, F. Meyer, *J. Am. Chem. Soc.* **2013**, *135*, 1704–1707.
- [38] T. R. Dugan, P. L. Holland, *J. Organomet. Chem.* **2009**, *694*, 2825–2830.
- [39] S. F. McWilliams, B. Q. Mercado, K. C. MacLeod, M. S. Fataftah, M. Tarrago, X. Wang, E. Bill, S. Ye, P. L. Holland, *Chem. Sci.* **2023**, *14*, 2303–2312.
- [40] J. P. Perdew, S. Kurth, A. Zupan, P. Blaha, *Phys. Rev. Lett.* **1999**, *82*, 2544–2547.
- [41] F. Weigend, R. Ahlrichs, *Phys. Chem. Chem. Phys.* **2005**, *7*, 3297–3305.

- [42] E. Caldeweyher, S. Ehlert, A. Hansen, H. Neugebauer, S. Spicher, C. Bannwarth, S. Grimme, *J. Chem. Phys.* **2019**, *150*, 154122.
- [43] L. Yan, C. H. Dapper, S. J. George, H. Wang, D. Mitra, W. Dong, W. E. Newton, S. P. Cramer, *Eur. J. Inorg. Chem.* **2011**, 2064–2074.
- [44] D. L. M. Suess, J. C. Peters, *J. Am. Chem. Soc.* **2013**, *135*, 12580–12583.
- [45] A. Klose, J. Hesschenbrouck, E. Solari, M. Latronico, C. Floriani, N. Re, A. Chiesi-Villa, C. Rizzoli, *J. Organomet. Chem.* **1999**, *591*, 45–62.
- [46] R. Hernández Sánchez, T. A. Betley, *J. Am. Chem. Soc.* **2015**, *137*, 13949–13956.
- [47] R. Hernández Sánchez, S.-L. Zheng, T. A. Betley, *J. Am. Chem. Soc.* **2015**, *137*, 11126–11143.
- [48] W. Petz, B. Neumüller, *Z. Anorg. Allg. Chem.* **2007**, *633*, 2032–2036.
- [49] H. Sakaba, M. Yoshida, C. Kabuto, K. Kabuto, *J. Am. Chem. Soc.* **2005**, *127*, 7276–7277.
- [50] M. M. Deegan, J. C. Peters, *Chem. Commun.* **2019**, *55*, 9531–9534.
- [51] Y. Lee, I.-R. Jeon, K. A. Abboud, R. García-Serres, J. Shearer, L. J. Murray, *Chem. Commun.* **2016**, *52*, 1174–1177.
- [52] H. Beinert, R. H. Holm, E. Müncck, *Science* **1997**, *277*, 653–659.
- [53] T. A. Kent, B. H. Huynh, E. Müncck, *Proc. Natl. Acad. Sci. USA* **1980**, *77*, 6574–6576.
- [54] J. F. Torres, C. H. Oi, I. P. Moseley, N. El-Sakkout, B. J. Knight, J. Shearer, R. García-Serres, J. M. Zadrozny, L. J. Murray, *Angew. Chem. Int. Ed.* **2022**, *61*, e202202329.
- [55] N. T. Daugherty, J. Bacsa, J. P. Sadighi, *Organometallics* **2017**, *36*, 3171–3174.
- [56] H. Zheng, K. M. Langner, G. P. Shields, J. Hou, M. Kowiel, F. H. Allen, G. Murshudov, W. Minor, *Acta Crystallogr. Sect. D* **2017**, *73*, 316–325.
- [57] H. Andres, E. L. Bominaar, J. M. Smith, N. A. Eckert, P. L. Holland, E. Müncck, *J. Am. Chem. Soc.* **2002**, *124*, 3012–3025.
- [58] J. H. Davis, M. A. Beno, J. M. Williams, J. Zimmie, M. Tachikawa, E. L. Muetterties, *Proc. Natl. Acad. Sci. USA* **1981**, *78*, 668–671.
- [59] M. Tachikawa, E. L. Muetterties, *J. Am. Chem. Soc.* **1980**, *102*, 4541–4542.
- [60] M. R. Churchill, J. Wormald, J. Knight, M. J. Mays, *J. Am. Chem. Soc.* **1971**, *93*, 3073–3074.
- [61] M. Rowen Churchill, J. Wormald, *J. Chem. Soc. Dalton Trans.* **1974**, *0*, 2410–2415.
- [62] M. Tachikawa, R. L. Geerts, E. L. Muetterties, *J. Organomet. Chem.* **1981**, *213*, 11–24.
- [63] D. Mansuy, J. P. Lecomte, J. C. Chottard, J. F. Bartoli, *Inorg. Chem.* **1981**, *20*, 3119–3121.
- [64] V. L. Goedken, M. R. Deakin, L. A. Bottomley, *J. Chem. Soc. Chem. Commun.* **1982**, 607–608.
- [65] E. N. Bakshi, C. D. Delfs, K. S. Murray, B. Peters, H. Homborg, *Inorg. Chem.* **1988**, *27*, 4318–4320.
- [66] G. Rossi, V. L. Goedken, C. Ercolani, *J. Chem. Soc. Chem. Commun.* **1988**, 46–47.
- [67] C. Ercolani, M. Gardini, V. L. Goedken, G. Pennesi, G. Rossi, U. Russo, P. Zanonato, *Inorg. Chem.* **1989**, *28*, 3097–3099.
- [68] L. Galich, A. Kienast, H. Hückstädt, H. Homborg, *Z. Anorg. Allg. Chem.* **1998**, *624*, 1235–1242.
- [69] J. Francois, Halet, D. G. Evans, D. M. P. Mingos, *J. Am. Chem. Soc.* **1988**, *110*, 87–90.
- [70] M. D. Fryzuk, B. R. Lloyd, G. K. B. Clentsmith, S. J. Rettig, *J. Am. Chem. Soc.* **1994**, *116*, 3804–3812.
- [71] P. J. Bailey, R. A. Coxall, C. M. Dick, S. Fabre, L. C. Henderson, C. Herber, S. T. Liddle, D. Loroño-González, A. Parkin, S. Parsons, *Chem. Eur. J.* **2003**, *9*, 4820–4828.
- [72] S. Stoll, A. Schweiger, *J. Magn. Reson.* **2006**, *178*, 42–55.
- [73] “EasyMoss: A Python/PyQt5 User-Friendly Application for the Simulation of Mössbauer Spectra”: R. Garcia-Serres, *Zenodo* **2021**, <https://doi.org/10.5281/zenodo.5634948>.
- [74] SAINT, version 7.68 A; Bruker AXS: Madison, WI, **2009**.
- [75] SADABS, version 2008/1; Bruker AXS: Madison, WI, **2009**.
- [76] G. M. Sheldrick, *Acta Crystallogr. Sect. A* **2008**, *64*, 112–122.
- [77] G. te Velde, E. J. Baerends, *J. Comput. Phys.* **1992**, *99*, 84–98.
- [78] S. H. Vosko, L. Wilk, M. Nusair, *Can. J. Phys.* **1980**, *58*, 1200–1211.
- [79] A. D. Becke, *Phys. Rev. A* **1988**, *38*, 3098–3100.
- [80] J. P. Perdew, *Phys. Rev. B* **1986**, *33*, 8822–8824.
- [81] P. J. Stephens, F. J. Devlin, C. F. Chabalowski, M. J. Frisch, *J. Phys. Chem.* **1994**, *98*, 11623–11627.
- [82] E. van Lenthe, A. Ehlers, E.-J. Baerends, *J. Chem. Phys.* **1999**, *110*, 8943–8953.
- [83] E. van Lenthe, E. J. Baerends, J. G. Snijders, *J. Chem. Phys.* **1993**, *99*, 4597–4610.
- [84] E. van Lenthe, R. van Leeuwen, E. J. Baerends, J. G. Snijders, *Int. J. Quantum Chem.* **1996**, *57*, 281–293.
- [85] E. van Lenthe, E. J. Baerends, J. G. Snijders, *J. Chem. Phys.* **1994**, *101*, 9783–9792.
- [86] E. van Lenthe, J. G. Snijders, E. J. Baerends, *J. Chem. Phys.* **1996**, *105*, 6505–6516.
- [87] G. L. Stoychev, A. A. Auer, F. Neese, *J. Chem. Theory Comput.* **2017**, *13*, 554–562.
- [88] M. Oriol, J.-M. Mouesca, *Inorg. Chem.* **2008**, *47*, 5394–5416.
- [89] P. Giannozzi, S. Baroni, N. Bonini, M. Calandra, R. Car, C. Cavazzoni, D. Ceresoli, G. L. Chiarotti, M. Cococcioni, I. Dabo, A. D. Corso, S. de Gironcoli, S. Fabris, G. Fratesi, R. Gebauer, U. Gerstmann, C. Gougaud, A. Kokalj, M. Lazzeri, L. Martin-Samos, N. Marzari, F. Mauri, R. Mazzarello, S. Paolini, A. Pasquarello, L. Paulatto, C. Sbraccia, S. Scandolo, G. Sclauzero, A. P. Seitsonen, A. Smogunov, P. Umari, R. M. Wentzcovitch, *J. Phys. Condens. Matter* **2009**, *21*, 395502.
- [90] J. P. Perdew, K. Burke, M. Ernzerhof, *Phys. Rev. Lett.* **1996**, *77*, 3865–3868.
- [91] Deposition numbers 2242876, 2242877, 2242878, 2242879, 2242880, and 2242881 contain the supplementary crystallographic data for this paper. These data are provided free of charge by the joint Cambridge Crystallographic Data Centre and Fachinformationszentrum Karlsruhe Access Structures service.

Manuscript received: June 23, 2023

Accepted manuscript online: August 18, 2023

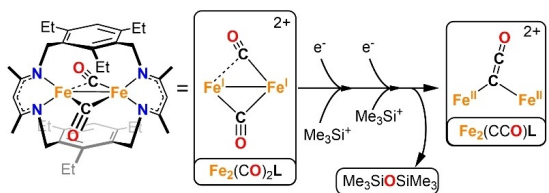
Version of record online: ■■■

Research Articles

Bioorganometallic Chemistry

D. Singh, B. J. Knight, V. J. Catalano,
R. García-Serres,* V. Maurel,* J.-
M. Mouesca,* L. J. Murray* – e202308813

Partial Deoxygenative CO Homocoupling
by a Diiron Complex



A diiron of a bis(beta-diketiminate) cyclophane effects the partially deoxygenative homologation of two CO molecules by two sequential one-electron reduction and silylation reactions to

generate a ketenylidene ligand. The ketenylidene can be readily released from the complex along with retention of the dinuclear metal construct.